

Evaluation of Antibacterial and Cytotoxic Effects of Green Synthesized Titanium Dioxide Nanoparticles

Farzana Rashid^{1*}, Samrin Habib¹, Iqra Noshair¹, Sadia Wattoo¹, Abdullah Etezaz², Adila Sana¹, Zahra Ghulam Haider¹

¹Department of Zoology, Lahore College for Women University, Jail Road, Lahore 54000, Punjab, Pakistan

²Institute of microbiology, University of Agriculture, Faisalabad

Abstract- The rise of antibiotic-resistant bacteria poses significant health challenges, leading to drug treatment failures. Titanium dioxide (TiO₂) nanoparticles (NPs) possess unique properties such as antibacterial, cytotoxic, optical, catalytic characteristics. This study synthesizes TiO₂ NPs using *Calotropis procera* leaf extract having particles size 10-50 nm. Antimicrobial efficacy was assessed against gram-negative and gram-positive bacteria using Kirby's disc diffusion assay at various concentrations. Cytotoxicity on cancer cell lines was evaluated via MTT assay and histological examinations determined the impact of TiO₂ NPs on kidney and liver tissues of albino mice. The study found increased serum biochemical parameters (ALT, AST, ALP, urea), while creatinine and total bilirubin levels were significantly decreased ($p < 0.005$). Maximum inhibition zones were observed at 40mg/ml, with antibacterial activity ranked as *S. aureus* > *E. coli* > *K. pneumoniae* > *E. faecalis*. Toxicity increased with higher nanoparticle concentrations, evidenced by cell swelling, hepatocyte necrosis, glomerulus degeneration, and nephritic tubule damage. The green-synthesized TiO₂ NPs showed effective antibacterial agents for future biomedical applications.

Index Terms- Titanium dioxide, *Calotropis procera*, Antibacterial, HepG2, MTT assay

I. INTRODUCTION

Nanoscience is a well-known branch of science that deals with the essential properties of nanoparticles. A vast spectrum of immediate therapeutic and anti-microbial possibilities in nanotechnology has emerged. Due to its extraordinary physicochemical and morphological characteristics, it is also being used in numerous disciplines, including biomedicine, biosensing, MRI, targeted drug delivery, phytopathology, and agriculture biotechnology [1,2]. Moreover, the high surface-to-volume ratio, high catalytic activity and excellent adsorption ability are the unique properties of nanoparticles [3]. Based on these characteristics, several biogenic manufactured nanoparticles like Titanium, Iron oxide, Copper, Gold, and Silver are used as anticancer and antifungal agents in a variety of sectors [4,5]. Microbial illnesses have been the primary cause of death and resistant bacteria are endangering global public health day by day [6]. Presently, multidrug-resistant (MDR) tuberculosis is the main reason that causes about 230,000 of the 700,000 annual deaths due to resistant infections.

By 2050, it is anticipated that drug-resistant illnesses will result in 10 million fatalities annually [7]. The plentiful dispersion of fungus spores in the soil and the air is also responsible for the remarkable rise in the incidence of fungal illnesses over the past several decades [8].

To overcome antibiotic resistance, the development of novel medications and advanced strategies are required [6,9]. The WHO strongly focuses on developing new antibiotics to combat diseases with resiliency [10]. Over the past ten years or more, there has been a significant increase in the risk of biological and bacterial attacks, particularly in areas that are used for human consumption, like food, food packaging, and water. Scientists are motivated by the rising risk to create new, risk-free, and simple-to-use inorganic antibacterial nanoparticle compounds [11]. This makes it possible for researchers to examine the advantages of nanomaterials in a variety of sectors, including biology, optoelectronics and the environment. Inorganic and organic nanoparticles are the two main categories of nanoparticles. At the beginning of the 20th century, various traditional techniques, such as chemical and physical procedures, were employed for the manufacture of nanoparticles [12]. These techniques weren't thought to be eco-friendly because of their toxicity and high expense, among other drawbacks. As a result, due to their eco-friendliness, therapeutic adaptability, stability and affordability, scientists and researchers are now showing a surprising interest in the production of metal oxide and metal nanoparticles using plants and biological organisms like bacteria, algae, and fungi [13]. According to the literature, different metal oxide and metal nanoparticles have been created utilizing plants and other living things [14]. So, in the realm of nanotechnology and nano-structure, biologically inspired technology for nanoparticle preparation has emerged as a wonderful and excellent field [15]. *Calotropis procera* (family Apocynaceae), is utilized in conventional treatments for the skin, lungs, stomach, and liver. Additionally, it possesses antibacterial and antiviral properties [16]. It is a xerophytic perennial shrub (or small tree) with tap roots that extend 3 to 4 meters into the ground and stems that are 2 to 6 meters tall. *C. procera* can withstand varying levels of soil salinity, drought stress and severe settings with bright light. It can also grow on a variety of soils. As a result, it is found in many tropical and subtropical regions [17]. *C. procera* posse's different kinds of phytochemicals, such as triterpenoids, flavonoids, glycosides, anthocyanins, α -amyrin, β -amyrin, lupeol, β -sitosterol, flavonols, mudarine and resins as well [18]. When compared to manufactured antimicrobials, phytochemicals

are thought to have no or fewer negative effects since they have varying degrees of effectiveness against microbial pathogens [19]. Some phytochemicals can break the cycle of antimicrobial resistance, alter it, or work in concert with traditional antibiotics. Indeed, there are various methods through which phytochemicals can act as antibacterial agents [7].

Due to their availability, affordability, high surface area-to-volume ratio, non-toxicity, and distinctive physiochemical properties, TiO₂ nanoparticles (TiO₂ NPs) are regarded as the material of choice in biological and environmental remediation applications among other metal oxide semiconductors like ZnO, MgO, CuO, and Fe₂O₃. TiO₂ nanoparticles' capacity to kill bacteria depends on the size, stability, and concentration of the growing medium they are put into. This increases the amount of time bacteria and nanoparticles have to interact, allowing them to contact closely with microbial membranes [20,21]. Additionally, it possesses a distinctive photocatalytic activity, strong thermal stability, and chemical biocompatibility. It is well known that the size, shape, and surface chemistry of TiO₂ nanoparticles, such as the number of surface flaws, have a major impact on the particles' photocatalytic activity and exhibit high antibacterial activity [22,23]. Plant-mediated nano-fabrication is a new area of nanotechnology that is favoured over traditional methods due to its properties of safety, affordability, environmental friendliness and biocompatibility.

The abundantly produced TiO₂ NPs are utilized regularly as a white pigment in the production of paintings, foods, paper, and toothpaste. Despite having a wide variety of functions, there is a lack of information on the impact of NPs on animal and human health [24]. The study aims to develop an eco-friendly and cost-effective synthesis of TiO₂ NPs in order to use them as antibacterial and anti-cancerous agents. In the present study, green synthesized TiO₂ NPs by *C. Procera* have been utilized for the first time against phytopathogens, which can give a thorough understanding of the anti-bacterial activity and cytotoxic effects of the synthesized NPs.

II. MATERIALS AND METHODS

2.1. Materials

Leaves of *Calotropis procera* (common name "Aak") for the preparation of extract were collected from the District Lahore. The plant leaves were recognized and authenticated by the Botany Department of Lahore College for Women University, Lahore.

2.2. Chemicals

Titanium tetra isopropoxide [Ti{(OCH(CH₃)₂)₄, Sigma Aldrich] was used as a precursor. The antibacterial activity of TiO₂ NPs was investigated by utilizing bacterial culture media such as Nutrient agar, Nutrient broth and Muller Hinton agar (Sigma-Aldrich). The antibiotics imipenem (10µg) and ciprofloxacin (5µg) (Bioanalyse Ltd. Ankara, Turkey) were utilized in this study. DMSO was used to make NP concentrations.

2.3. Preparation of Plant Extract

The fresh leaves of *C. procera* were rinsed multiple times to eradicate dust particles. After washing, the leaves were dried in the shade for 2-3 days. Weighing 50g of dried finely chopped leaves and dipped in 100 ml of sterilized distilled water. The mixture was boiled for 60 min until the colour of the aqueous solution changed to

light yellow. The extract was filtered using Whatman No. 1 filter paper and stored at room temperature to be used for further experiments.

2.4. Green Synthesis of TiO₂ NPs

40ml prepared *C. procera* leaves aqueous extract and 10 ml titanium tetra isopropoxide were mixed with 300 ml distilled water. The mixture was transferred on a magnetic stirrer at room temperature for 2 hours, as described in our previous study by Habib *et al.* [25]. After that, the mixtures were sonicated for 30 min and then filtered by using filter paper and remained as such to dry. After that, dried material was collected and ground in a mortar pestle to obtain fine particles.

2.5. Characterization of TiO₂ NPs

Characterization of synthesized TiO₂ NPs using *C. procera* leaves extract, including a combination of spectroscopic techniques such as UV-visible spectroscopy (UV-Vis), X-ray diffraction (XRD), Fourier transform infrared (FTIR) spectroscopy and Scanning Electron Microscopy (SEM) was conducted as described in our previous paper Habib *et al.* [25] to analyze their structure, composition, size and crystallinity.

2.6. Bacterial Strains

Non-repetitive twenty (20) bacterial strains were collected from General Hospital, Lahore. All bacterial strains were collected from samples of different patients (pus, ear sap, wound, etc.), and different morphological and biochemical tests (Citrate, indole, etc.) were performed to characterize bacterial strains. Only those bacterial strains were selected which showed beta-lactamase activity. These selected strains were used from ATCC, such as *Staphylococcus aureus* (*S. aureus*, 29213), *Escherichia coli* (*E. coli*, 25922), *Klebsiella pneumonia* (*K. pneumonia*, 23101), and *Enterococcus faecalis* (*E. faecalis*, 14508) and all these strains were sensitive to imipenem and resistant to ciprofloxacin.

2.6. Antibacterial Activity of TiO₂ NPs

The antibacterial activity of *C. procera* leaves extract and TiO₂ NPs was evaluated by the Kirby-Bauer disc diffusion method [26]. Antibacterial activity against gram-negative and gram-positive bacteria was determined using various concentrations of green synthesized TiO₂ NPs (10, 20, 30 and 40mg/ml) and extract. Freshly prepared cultures of tested organisms were uniformly spread with sterilized cotton swabs on the Muller Hinton plate. Standard Whatman filter paper discs impregnated with TiO₂ NP concentrations, antibiotics (imipenem and ciprofloxacin) as positive control and saturated discs with water as negative control were applied on the prepared Muller Hinton plates. After 24 hrs incubation, ZOI was recorded in mm at room temperature (30°C). An experiment was performed in triplicates at room temperature including UV light.

2.7. Cytotoxic Effect of TiO₂ NPs on Cancer Cell lines

Cytotoxic effects and biocompatibility of green synthesized TiO₂ NPs were measured by using a HepG2 cancer cell line.

2.7.1. Cell Culturing

HepG2 (ATCC HB-8065™) human hepatocellular carcinoma cells were obtained from the American Type Culture Collection (Manassas, VA, United States) and cultured as monolayer in T-75 flasks Costar, followed by subculturing twice a week at 37°C in 5%

CO₂ and 100% relative humidity supplied incubator at a density of 1×10^5 . HepG2 was cultured in McCoy's 5A medium Gibco Glasgow, supplemented with 10% fetal bovine serum FBS, Gibco, Glasgow, UK and 1% antibiotics (streptomycin, penicillin). The experiment was performed in triplicates at the University of Lahore.

2.7.2. MTT Assay

The cell viability of the HepG2 cancer cells line treated with biosynthesized TiO₂ NPs was assessed by using 3-(4, 5-dimethylthiazol-2-yl)-2, 5-diphenyl tetrazolium bromide (MTT) yellow dye. Furthermore, HepG2 cancer cells were seeded in the 96-microtitre plate at densities of 1×10^4 cells per well and kept in the CO₂ incubator for 24h for adherence. Then, the Cells were treated with different concentrations of biosynthesized TiO₂ NPs such as 10 µg/ml, 50 µg/ml, 100 µg/ml, 200 µg/ml and *C. procera* leaves extract and plate were incubated for another 24 h. An experiment was performed in triplicates to avoid any errors, according to Al-Shabib *et al.* [27], with little modifications. After 24 h, 25 µL MTT was added to each well and kept the plate for 4 h in the incubator. After discarding the supernatant, 100 µL DMSO was added to each well for the dissemination of crystals and absorbance was read at 550 nm.

The below formula calculated cytotoxicity and cell viability.

$$\text{Cytotoxicity} = [(Control - Treated) / Control] \times 100$$

$$\text{Cell viability} = (Treated / Control) \times 100$$

2.8. In Vivo studies

2.8.1 Ethical Approval

Approval for the experiment was obtained from the ethical review committee of Lahore College for Women University, Lahore, via RERC No/LCWU/ZOO/577 Dated 9 June 2022, and the execution followed in accordance.

2.8.2. Effects of Green Synthesized TiO₂ Nanoparticles on the Kidney of Mice

In vivo research was done to assess the toxic effects of green-synthesized TiO₂ NPs. From the University of Veterinary and Animal Sciences (UVAS), 7–8-week-old twenty-four (24) healthy albino mice (weight in average 25-30g) were purchased for the research purpose. They were then given standard circumstances, such as 12h light/dark cycle, 25 ± 5 °C temperature ranges, and were acclimated for 7 days. They were then fed a standard diet for the duration of the experiment and given free access to water and pellets. Experiments were performed in triplicate on healthy individuals as described by Noori *et al.*[28].

Two sets of animals were formed: a control group and an experimental group. Based on the dose that was administered to the animals, each experimental group was further divided into three sub-groups (each sub-group comprises 6 individuals). The control group received feed and saline solution in addition to the experimental group was given low (100 mg/kg bw), medium (200 mg/kg bw), and high doses (300 mg/kg bw) TiO₂ NPs orally via gavage for 7, 14, and 21 days.

2.8.1. Histological Examinations

Under ether anaesthesia, dissection was performed after 7, 14 and 21 days, and blood samples were obtained through cardiac puncture. Excision and weighing of the liver and kidneys took place, and the fractional contributions of these organs were determined as the ratio

of wet tissue weight (mg) to body weight (g). Kidney and livers were immediately transferred to a fixation solution (10% formalin) for further histological examination. Sections with a thickness of approximately 5 µm were cut using a rotatory microtome, stained with haematoxylin and eosin, and observed for histopathological changes under a microscope equipped with a digital camera (B-150 Optika, Italy) at 40X magnification.

2.9. Statistical Analysis

All the experiments, including antibacterial and cytotoxic activity, were carried out in triplicates. The data was evaluated, and results are presented as means \pm standard deviation by using Microsoft Excel version (2013). Analysis of Variance (ANOVA) was used to describe the difference between means of the parameter in the treated and control group ($p < 0.05$).

III. RESULTS

3.1. Characterizations of TiO₂ NPs

Green synthesized TiO₂ NPs from the leaves of *C. Procera* were characterized by UV spectroscopy, XRD, FTIR and SEM for average crystalline size, average particle size, optical properties and thermal stability. The optical properties of the nanoparticles are studied using a UV-visible spectrophotometer. Figure (1) depicts the TiO₂ NPs' absorption spectrum, which spans the 200–800 nm regions. The absorbance peak of TiO₂ was visible at 285 nm. The lack of any other peak in the region of the absorption spectrum served as a measurement of the purity of TiO₂ NPs. A novel method for determining the structure and crystalline size of the nanoparticles is X-ray diffraction. The XRD pattern of green synthesized TiO₂ NPs displayed in Figure (2). As shown in Figure 2, the spectrum of the TiO₂ XRD pattern is between the diffraction angles $20 < 2\theta < 80$. Figure 2 depicts the various TiO₂ peaks with good agreement with the JCPDS card (21-1272) at angles of 27.52°, 37.36°, 48°, 54.75°, 62.19° and 74°, which correlate to (110), (004), (200), (211), (213), and (301). The peak's position and the absence of an additional peak in the diffraction pattern both verified the integrity of the TiO₂ NPs. The breadth of the peak and the size of the NPs are inversely correlated; as the peak width increases, the size of the NPs decreases. FTIR The peak of a sample is used to analyze the functional behavior of the sample using FT-IR spectroscopy. Because each compound in the NPs has a distinct atomic rearrangement, each compound displayed a distinct IR pattern. Green synthesized TiO₂ NPs were analyzed by FTIR spectroscopy, which showed that distinct functional groups were present and were detected at various wavelengths. *C. Procera* leaves were used to make TiO₂, and Figure (3) shows that the FT-IR band in the 100% transmittance mode ranges from 4000 to 500 cm⁻¹. Scanning electron microscopy (SEM) was used to illustrate the size and shape of TiO₂ NPs, as shown in Figures (4). SEM micrographs showed the individual and number of aggregates. The micrograph reveals that irregular shape TiO₂ NPs were formed with diameter range 10-35nm. The Figure 4 indicated that smaller size TiO₂ NPs were formed with an average size 18nm. Because these NPs contain a variety of secondary compounds, including alkaloids, peptides, terpenoids, polyphenols, and flavonoids, they function as reducing agents. By altering the morphology of the NPs, the complete set of properties and behavior fluctuates.

3.2. Antibacterial Effects of Green Synthesized TiO₂ NPs

Disk diffusion assay was used to study the antibacterial activity of TiO₂ NPs against gram-positive and gram-negative bacteria.

Different concentrations of TiO₂ NPs, i.e. 10 mg/ml, 20 mg/ml, 30 mg/ml and 40 mg/ml, were used, and the zones of inhibition (ZOI) formed were measured after 24h. Figure (5,6) and Table (1) describe the ZOI formed at various concentrations and their measurements, respectively. The synthesized TiO₂ NPs exhibited stronger antibacterial activity. Maximum inhibition zones were observed in gram-positive bacteria (*S. aureus*), and minimum ZOI was observed in negative bacteria (*E. faecalis*).

3.3. MTT Assay

MTT assay was used to determine the cytotoxicity of *C. Procera* leaves extract and TiO₂ NPs on HepG2 liver cancer cell lines. The effect on HepG2 cells exposed to different TiO₂ NP concentrations (10–200 µg/mL) and the extract is depicted in terms of cell viability (%) as shown in Table 2. TiO₂ NPs induced a concentration-dependent decrease in the cell viability of HepG2. Cell viability was recorded as 90.9%, 75%, 60.6%, and 53.7% at 10, 50, 100, and 200 µg/mL concentrations, respectively, using MTT assay (Figure 7). 76% of cells were alive when the cell was treated with *C. Procera* leaves extract.

3.4. Effects of TiO₂ Nanoparticles on the Liver and Kidney

3.4.1. Coefficients of Liver and Kidneys

After 7, 14 and 21 days, the mice were sacrificed, and the weight of the body and various tissues/organs were collected. Table 3 shows the coefficients of the liver and kidneys to body weight, which are expressed as milligrams (wet weight of tissues)/g (body weight).

3.4.2. Biochemical Parameters in Serum

Liver function was evaluated with serum levels of alkaline phosphatase (ALP), aspartate aminotransferase (AST), Alanine transaminase (ALT) and total bilirubin (TBIL) level. Nephrotoxicity is determined by serum levels of uric acid (UA), blood urea nitrogen (Urea), and creatinine (CR). All biochemical assays were performed using a fully automated, random access, dry Biochemistry analyzer (Vitros-250, Johnson and Johnson Co., NY, USA).

In the male albino mice, after 7 days of exposure to different-sized green synthesized TiO₂ NPs, the ALP/ALT/AST level was slightly elevated and significantly increased after 14 and 21 days. The higher serum Urea and CR levels were found in the male albino mice exposed to the different concentrations (100, 200, and 300 mg/ml) of TiO₂ NPs after 7, 14 and 21 days. Table 4 shows the changes in biochemical parameters in the serum of male albino mice induced by TiO₂ NPs. There are significant changes for the enzymes of ALT, AST and ALP ($p > 0.05$) after oral administration of different sized TiO₂ NPs. However, the TBIL and UA levels were decreased after exposure to TiO₂ NPs in the three experimental groups compared with the control group.

3.4. Effects of TiO₂ Nanoparticles on the Kidney

Histological Examination

In this particular investigation, animals were subjected to varying doses (100mg/kg, 200mg/kg and 300mg/kg body weight) of TiO₂ NPs administered orally for 7, 14 and 21 days. Following different time intervals (7, 14 and 21 days), the animals were euthanized to examine the acute and chronic toxicological effects of TiO₂. After 7, 14, and 21 days of exposure, kidney and liver tissues induce changes due to the presence of TiO₂ NPs at different concentrations (100 mg/kg, 200 mg/kg, and 300 mg/kg body weight). Kidney sections 8(A) from the control group exhibited normal renal cortex and normal nephritic tubules. In contrast, the second group treated with

(100 mg/kg body weight/day) displayed pathological abnormalities, including a slight expansion in the collecting tubules of the medulla and normal renal cortex, as shown in Figure 8(B). The third group, which received (200 mg/kg body weight/day) of TiO₂ NPs, exhibited inflammation characterized by the accumulation of mononuclear cells around blood vessels and between renal tubules in the kidney, as represented in Figure 8(C). The fourth group, treated with 300 mg/kg, showed severe toxic effects such as cell destruction, increased intracellular spaces, and distorted glomeruli, as presented in Figure 8(D).

Histological sections from the liver of the control group Figure 9(A) revealed normal hepatocytes, eosinophilic cytoplasm and central vein. Liver section from albino mice exposed to 100 mg/kg body weight of TiO₂ NPs (low dose) showed almost normal histology with hepatocytes similar in appearance to the control group with a prominent nucleus and eosinophilic cytoplasm after 7 and 14 days and only mild infiltration of the central vein was observed after 21 days exposure and shown in Figure 9 (B). Albino mice exposed to 200 and 300 mg/kg body weight of TiO₂ NPs (medium dose) revealed liver sections with central vein infiltration, hepatocytes with reduced eosinophilic and liver sinusoid dilation was observed after 21 days, and swelling of the central vein was also observed after 21 days and shown in Figure 9(C, D).

IV. DISCUSSION

Due to the increasing demand for low-cost methods, nontoxic chemicals, antibacterial, antiviral, diagnostic, anticancer, targeted drug delivery, environmentally friendly solvents, and reusable materials over the past few years, biosynthesis of nanoparticles has attracted considerable attention [29]. TiO₂ NPs have great applications in the areas of photocatalysts, cosmetics, and pharmaceuticals. The area of interaction between nanoparticles and pathogenic bacteria increases due to small-size NPs, making them ideal as antimicrobial agents. Due to their small size, the particles can readily enter bacterial surfaces and cause damage [30]. Due to its low cost as compared to other noble metals like Au, Pt and Ag, TiO₂ nanoparticles have gained popularity among researchers.

The present research work was designed to synthesize TiO₂ NPs from leaves of *C. procera* and to evaluate the antimicrobial effects of leaves extract and TiO₂ NPs by disc diffusion method against gram-negative and gram-positive bacterial strains, i.e. *E. coli* and *K. pneumoniae*, *S. aureus* and *E. faecalis*. All of the bacterial strains used were sensitive to β -lactam antibiotic imipenem while resistant to antibiotic ciprofloxacin. The antimicrobial effect of leaf extract and TiO₂ NPs with four concentrations (10 mg/ml, 20 mg/ml, 30 mg/ml and 40 mg/ml) was checked individually, and with antibiotics against bacterial strains, the result reveals that ZOI increased as the concentration of TiO₂ NPs was increased.

The toxicity level of TiO₂ NPs was also evaluated in the kidneys of male albino mice. The mice were treated with three different concentrations of low dose (100mg/kg), medium dose (200mg/kg) and high dose (300mg/kg) of NPs. It was observed that these small-sized TiO₂ NPs can damage kidney tissues. The toxicity of NPs in the kidney of mice varied according to the dose. A high level of toxicity was evaluated in mice that were treated with a high dose when compared to a low dose, and no toxicity was observed in the control group that was injected with saline water. Histological changes were observed in mice kidney that induces degeneration, swelling and shrinkage of glomeruli. The capsular space in the renal cortex was also increased according to the concentration of NPs that was given to the mice. It was shown that cellular space between the

cells increased, and in the high-dose treated group, oedema formation was observed in the cells.

A similar study was conducted by Noori et al. [28] that supports our results. They also checked the effect of TiO₂ NPs on the kidneys of mice. They grouped the animals into 16 groups of 8 in each. The experiment lasted 30 days. Animals were orally injected with NPs of different concentrations, low dose (100mg/kg) and high dose (300mg/kg) and were sacrificed after 8, 15, and 30 days of post-injection. At this point, our study shows similarity, that animals were sacrificed in 2 groups after 10 days and after 20 days of treatment. They observed structural changes in the kidney. These changes were swelling of glomerular fibrosis and necrosis. In our results, the same structural changes were observed.

The present study was designed to analyze the effect of TiO₂ NPs (100 mg/kg body weight and 300 mg/kg body weight) in liver tissue after 7, 14 and 21 days of exposure. Histological sections from the liver of the control group revealed normal hepatocytes, eosinophilic cytoplasm and central vein. After 14 and 21 days, low-dose exposure did not reveal any changes in normal histology, but a high dose after 10 days induced central vein infiltration and after 21 days, high-dose exposure swelling and infiltration of central vein and liver sinusoid dilation was observed. It means the toxicity of NPs in the liver of albino mice depends on the quantity of doses.

Similar research was conducted by Sharma et al. [31] that supports our findings that oral immediate exposure to TiO₂ NPs promotes apoptosis and severe oxidative stress in mouse liver cells. TiO₂ NPs can cause alterations in the kidney and liver tissues of albino male mice, according to histopathological research. Excess TiO₂ NPs in the diet may cause liver damage. Sana et al. [32] found that the histo-toxicity of TiO₂ NPs in renal and liver tissues was higher at high doses (350 mg/kg body weight/ day) than at low doses (150 mg/kg body weight/ day).

Brunner et al. [33] found that TiO₂ NPs impact the histology of the liver and kidney, particularly at higher doses and, to a lesser extent, at medium doses. The rise in divalent Titanium ions level following dissolution is thought to be the cause of TiO₂ NPs' cytotoxicity. It may be inferred that when Ti is administered *in vivo*, it dissolves as divalent Zn ions, creating a rise in the ionic zinc form. As a result, the previous histological effects were seen. TiO₂ NPs accumulate in the liver, which is the body's biggest detoxifying organ, and may cause reactive oxygen species. Other nanoparticles can use similar oxidative processes to exert hazardous effects.

V. CONCLUSION

The present research work revealed that green synthesized TiO₂ NPs by using *Calotropis procera* leaf extract inhibit the growth of gram-negative and gram-positive at different concentrations. TiO₂ NPs showed significant antimicrobial activity against all the tested microorganisms. Results showed that TiO₂ NPs are more susceptible to gram-negative bacteria and may be considered as potent antimicrobial agents for drug-resistant bacterial strains. Antibacterial activity and cytotoxicity of TiO₂ NPs increases with the increase in concentration of nanoparticles. The synthesized NPs induced considerable reduction in the viability of HepG2 *in vitro* and could prove effective in controlling liver cancer. In summary, the green synthesized TiO₂ NPs demonstrate diverse biological properties, could be used as an anti-bacterial agent and for cancer cells treatment.

ACKNOWLEDGMENT

The authors extend their appreciation to Department of Biotechnology, University of Lahore and institute of microbiology, University of Agriculture, Faisalabad for providing facilities for some part of research work.

REFERENCES

- [1] Khalil, A. T., Khan, M. D., Razzaque, S., Afridi, S., Ullah, I., Iqbal, J., & Ayaz, M. (2021). Single precursor-based synthesis of transition metal sulfide nanoparticles and evaluation of their antimicrobial, antioxidant and cytotoxic potentials. *Applied Nanoscience*, 11(9), 2489-2502.
- [2] Shah, I. H., Ashraf, M., Sabir, I. A., Manzoor, M. A., Malik, M. S., Gulzar, S., & Zhang, Y. (2022). Green synthesis and Characterization of Copper oxide nanoparticles using *Calotropis procera* leaf extract and their different biological potentials. *Journal of Molecular Structure*, 1259, 132696.
- [3] Abbasi, B. A., Iqbal, J., Kiran, F., Ahmad, R., Kanwal, S., Munir, A., ... & Mahmood, T. (2020). Green formulation and chemical characterizations of *Rhamnella gilgitica* aqueous leaves extract conjugated NiONPs and their multiple therapeutic properties. *Journal of Molecular Structure*, 1218, 128490.
- [4] Cai, F., Li, S., Huang, H., Iqbal, J., Wang, C., & Jiang, X. (2022). Green synthesis of gold nanoparticles for immune response regulation: Mechanisms, applications, and perspectives. *Journal of Biomedical Materials Research Part A*, 110(2), 424-442.
- [5] Iqbal, J., Abbasi, B. A., Ahmad, R., Mahmoodi, M., Munir, A., Zahra, S. A., ... & Capasso, R. (2020). Phytogetic synthesis of nickel oxide nanoparticles (NiO) using fresh leaves extract of *Rhamnus triquetra* (wall.) and investigation of its multiple *in vitro* biological potentials. *Biomedicines*, 8(5), 117.
- [6] Khameneh, B., Iranshahy, M., Soheili, V., & Fazly Bazzaz, B. S. (2019). Review on plant antimicrobials: a mechanistic viewpoint. *Antimicrobial Resistance & Infection Control*, 8(1), 1-28.
- [7] Biharee, A., Sharma, A., Kumar, A., & Jaitak, V. (2020). Antimicrobial flavonoids as a potential substitute for overcoming antimicrobial resistance. *Fitoterapia*, 146, 104720.
- [8] Vidyasagar, G.M., 2016. Plant-derived antifungal agents: Past and recent developments. In: Basak, A., Chakraborty, R., Mandal, S. M. (Eds.), *Recent Trends in Antifungal Agents and Antifungal Therapy*. Springer India, pp. 123-147.
- [9] Mulat, M., Khan, F., Muluneh, G., and Pandita, A. (2020). Phytochemical profile and antimicrobial effects of different medicinal plant: current knowledge and future perspectives. *Current Traditional Medicine*, 6(1), 24-42.
- [10] World Health Organization. (2017). *Antibacterial agents in clinical development: an analysis of the antibacterial clinical development pipeline, including tuberculosis* (No. WHO/EMP/IAU/2017.11). World Health Organization.
- [11] Khashan, K. S., Sulaiman, G. M., Abdulameer, F. A., Albukhaty, S., Ibrahim, M. A., Al-Muhimeed, T., & Al-Obaid, A. A. (2021). Antibacterial activity of TiO₂ nanoparticles prepared by one-step laser ablation in liquid. *Applied Sciences*, 11(10), 4623.
- [12] Ahmed, S., Ahmad, M., Swami, B. L., & Ikram, S. (2016). A review on plants extract mediated synthesis of silver nanoparticles for antimicrobial applications: a green expertise. *Journal of Advanced Research*, 7(1), 17-28.
- [13] Ijaz, I., Bukhari, A., Gilani, E., Nazir, A., Zain, H., & Saeed, R. (2022). Green synthesis of silver nanoparticles using different plants parts and biological organisms, characterization and antibacterial activity. *Environmental Nanotechnology, Monitoring & Management*, 18, 100704.
- [14] Vanlalveni, C., Lallianrawna, S., Biswas, A., Selvaraj, M., Changmai, B., & Rokhum, S.L. (2021). Green synthesis of silver nanoparticles using plant extracts and their antimicrobial activities: a review of recent literature. *RSC Adv.* 11 (5), 2804-2837.
- [15] Pathak, G., Rajkumari, K., & Rokhum, S. L. (2019). Wealth from waste: *M. acuminata* peel waste-derived magnetic nanoparticles as a solid catalyst for the Henry reaction. *Nanoscale Advances*, 1(3), 1013-1020.

- [16] Yaniv, Z., & Koltai, H. (2018). *Calotropis procera*, Apple of Sodom: Ethnobotanical review and medicinal activities. *Israel Journal of Plant Sciences*, 65(1-2), 55-61.
- [17] Hassan, L.M., Galal, T.M., Farahat, E.A., & El-midany, M.M. (2015). The biology of *Calotropis procera* (Aiton) W.T. *Trees – Struct. Funct.* 29 (2), 311–320. <https://doi.org/10.1007/s00468-015-1158-7>.
- [18] Mali, R. P., Rao, P. S., & Jadhav, R. S. (2019). A review on pharmacological activities of *Calotropis procera*. *Journal of Drug Delivery and Therapeutics*, 9(3), 947-951.
- [19] Amini, M. H., Ashraf, K., Salim, F., Lim, S. M., Ramasamy, K., Manshoor, N., ... & Ahmad, W. (2021). Important insights from the antimicrobial activity of *Calotropis procera*. *Arabian Journal of Chemistry*, 14(7), 103181.
- [20] Sánchez-López, E., Gomes, D., Esteruelas, G., Bonilla, L., Lopez-Machado, A.L., Galindo, R., Cano, A., Espina, M., Ettcheto, M., Camins, A., & Silva, A.M. (2020). Metal-based nanoparticles as antimicrobial agents: an overview. *Nanomaterials*, 10(2), 292.
- [21] Han, C., Romero, N., Fischer, S., Dookran, J., Berger, A., & Doiron, A. L. (2017). Recent developments in the use of nanoparticles for treatment of biofilms. *Nanotechnology Reviews*, 6(5), 383-404.
- [22] Albukhaty, S., Al-Karagoly, H., & Dragh, M. A. (2020). Synthesis of zinc oxide nanoparticles and evaluated its activity against bacterial isolates. *J. Biotech Res*, 11, 47-53.
- [23] Pan, Z., Lee, W., Slutsky, L., Clark, R.A., Pernodet, N., & Rafailovich, M.H. (2009). Adverse effects of titanium dioxide nanoparticles on human dermal fibroblasts and how to protect cells. *Small*, 5(4), 511-520.
- [24] Valentini, X., Rugira, P., Frau, A., Tagliatti, V., Conotte, R., Laurent, S., Colet, J.M., & Nonclercq, D. (2019). Hepatic and renal toxicity induced by TiO₂ nanoparticles in rats: a morphological and metabonomic study. *Journal of Toxicology*, 2019.
- [25] Habib, S., Rashid, F., Tahir, H., Liaqat, I., Latif, A.A., Naseem, S., Khalid, A., Haider, N., Hani, U., Dawoud, R.A., et al. Antibacterial and Cytotoxic Effects of Biosynthesized Zinc Oxide and Titanium Dioxide Nanoparticles. *Microorganisms*, 11, 1363. <https://doi.org/10.3390/microorganisms11061363>
- [26] Bauer, B. E., Lorenzetti, S., Miaczynska, M., Bui, D. M., Schweyen, R. J., & Ragnini, A. (1996). Amino- and carboxy-terminal domains of the yeast Rab escort protein are both required for binding of Ypt small G proteins. *Molecular biology of the Cell*, 7(10), 1521-1533.
- [27] Al-Shabib, N.A., Husain, F.M., Qais, F.A., Ahmad, N., Khan, A., Alyousef, A.A., Arshad, M., Noor, S., Khan, J.M., Alam, P., & Albalawi, T.H. (2020). Phyto-mediated synthesis of porous titanium dioxide nanoparticles from *Withania somnifera* root extract: broad-spectrum attenuation of biofilm and cytotoxic properties against HepG2 cell lines. *Frontiers in Microbiology*, 11, 1680.
- [28] Noori, A., Karimi, F., Fatahian, S., & Yazdani, F. (2013). Effects of Zinc Oxide nanoparticles on renal function in mice. *Journal of Kashan University of Medical Sciences*, 16 (7), 603-604.
- [29] Subhapiya, S. & Gomathipriya, P. (2018). Green synthesis of titanium dioxide (TiO₂) nanoparticles by *Trigonella foenum-graecum* extract and its antimicrobial properties. *Microbial Pathogenesis*, 116, 215-220.
- [30] Hudlikar, M., Joglekar, S., Dhaygude, M., & Kodam, K. (2012). Green synthesis of TiO₂ nanoparticles by using aqueous extract of *Jatropha curcas* L. latex. *Materials Letters*, 75, 196-199.
- [31] Sharma, P., Schaubel, D. E., Gong, Q., Guidinger, M., & Merion, R. M. (2012). End-stage liver disease candidates at the highest model for end-stage liver disease scores have higher wait-list mortality than status-1A candidates. *Hepatology*, 55(1), 192-198.
- [32] Sana, S.S., Badineni, V.R., Arla, S.K. and Boya, V.K.N. (2015) Eco-Friendly Synthesis of Silver Nanoparticles Using Leaf Extract of *Grewia flavescens* and Study of Their Antimicrobial Activity. *Materials Letters*, 145, 347-350. <https://doi.org/10.1016/j.matlet.2015.01.096>
- [33] Brunner, T. J., Wick, P., Manser, P., Spohn, P., Grass, R. N., Limbach, L. K., ... & Stark, W. J. (2006). In vitro cytotoxicity of oxide nanoparticles: comparison to asbestos, silica, and the effect of particle solubility. *Environmental science & technology*, 40(14), 4374-4381.

AUTHORS

First Author – Prof. Dr. Farzana Rashid, Department of Zoology, Lahore College for Women University, Lahore

Second Author – Samrin Habib, Ph.D scholar, Department of Zoology, Lahore College for Women University, Lahore ;

Third Author – Iqra Noshair, Ph.D scholar, Department of Zoology, Lahore College for Women University, Lahore; ORCID-0009-0006-8174-8652

Forth Author – Sadia Wattoo, Ph.D scholar, Department of Zoology, Lahore College for Women University, Lahore;

Fifth Author – Abdullah Etezaz, Ph.D scholar, Institute of microbiology, University of Agriculture, Faisalabad Pakistan;

Sixth Author – Adila Sana, MS scholar, Department of Zoology, Lahore College for Women University, Lahore;

Seventh Author – Zahra Ghulam Haider, MS scholar, Department of Zoology, Lahore College for Women University, Lahore;

Correspondence Author – Prof. Dr. Farzana Rashid

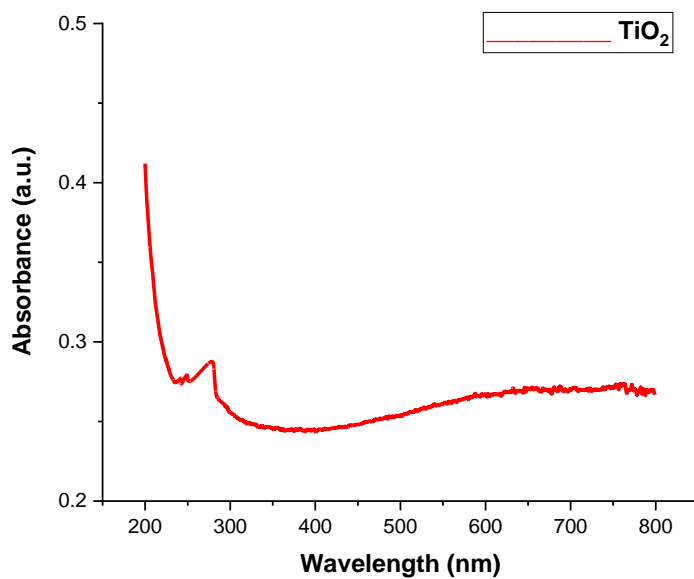


Figure 1. UV Visible Spectra of TiO₂ NPs

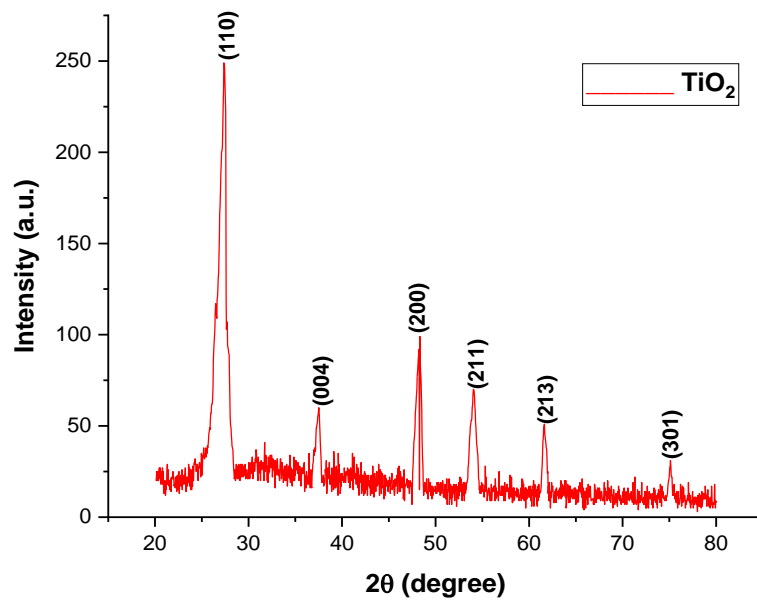


Figure 2. X-ray Diffraction of Green synthesized TiO₂ NPs

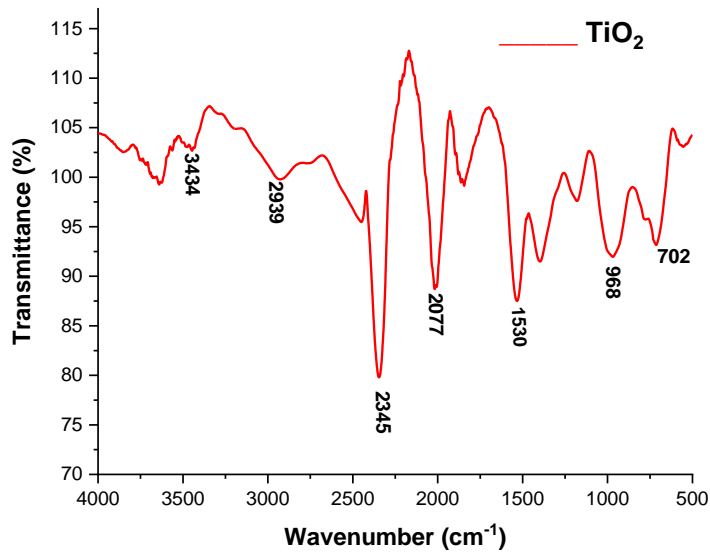


Figure 3. FTIR spectra of TiO₂ NPs

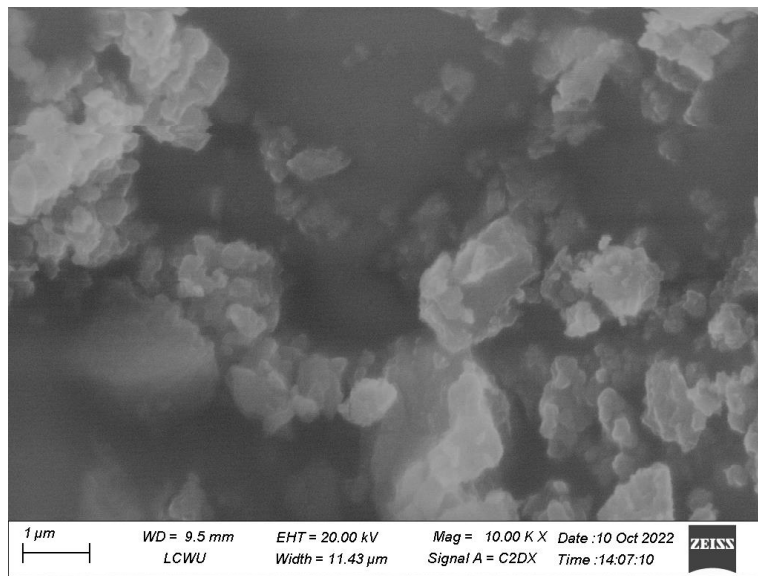


Figure 4. SEM of TiO₂ NPs



E. coli 79601

K. pneumoniae 358

S. aureus 328

E. faecalis 111

Figure 5. A: 10mg/ml B: 20mg/ml C: 30mg/ml D: 40mg/ml E: Negative Control (water paper disc) S: Sensitive bacteria to antibiotic (Imipenem) R: Resistant bacteria to antibiotic (Ciprofloxacin)

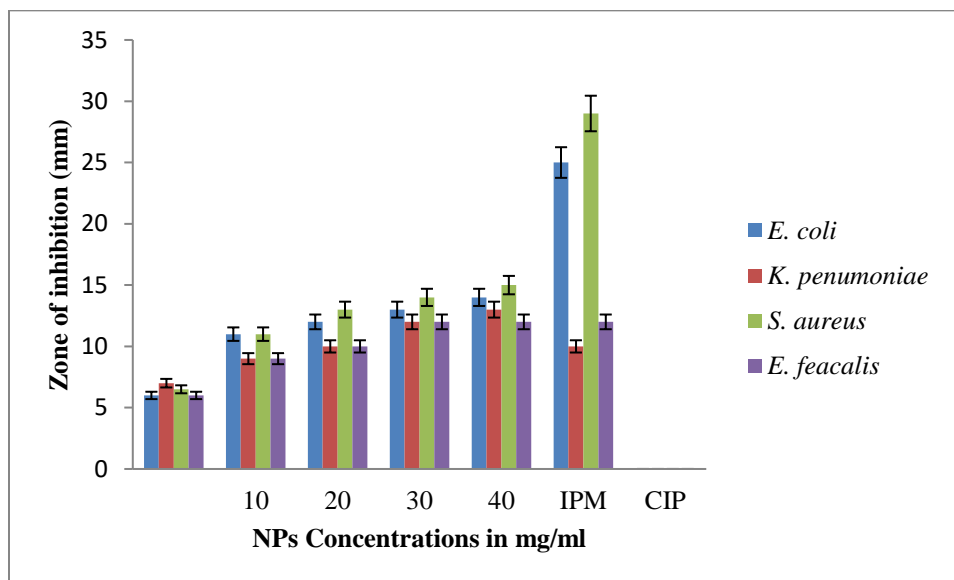


Figure 6. Antibacterial activity of TiO₂ NPs

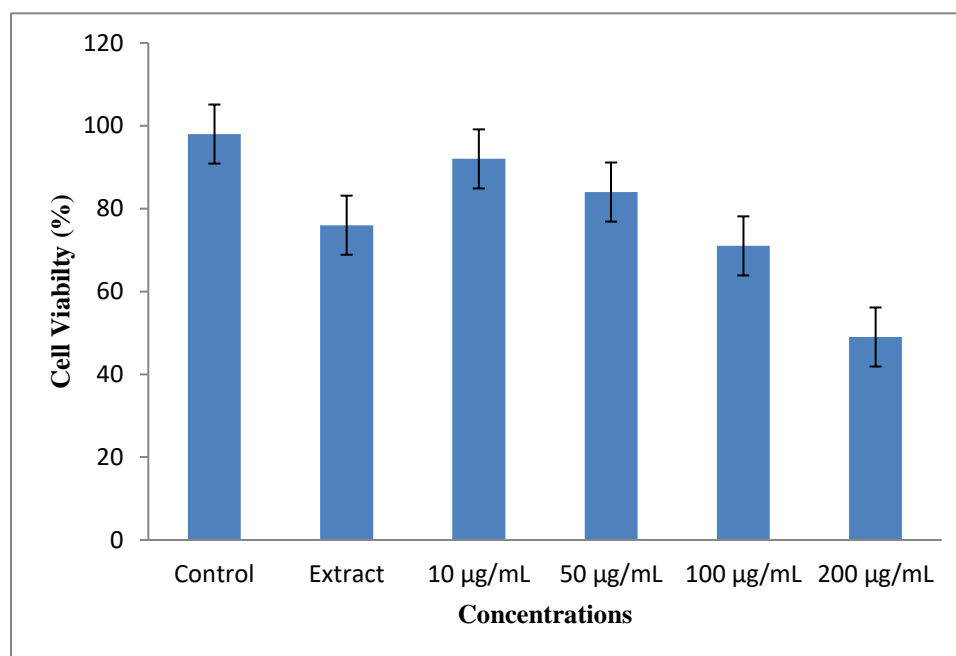
Table 1. Antibacterial activity of TiO₂ NPs by disc diffusion method

| Strains | Zone of inhibition in mm | | | | | | |
|----------------------|----------------------------------|--|--------|---------|---------|-------------|-----|
| | <i>C. procera</i> leaves extract | Concentration of TiO ₂ NPs (mg/ ml) | | | | Antibiotics | |
| | | 10 | 20 | 30 | 40 | IPM | CIP |
| <i>E. coli</i> | 6±0.2 | 11±0.2 | 12±0.5 | 13 ±0.8 | 14±0.3 | 25±0.7 | R |
| <i>K. pneumoniae</i> | 7±0.2 | 9±0.2 | 10±0.6 | 12 ±1 | 13 ±1.5 | 10±0.5 | R |
| <i>S. aureus</i> | 6.5±0.3 | 11±0.3 | 13±0.1 | 14 ±2 | 15 ±1 | 29±1.5 | R |
| <i>E. faecalis</i> | 6±0.2 | 9±0.2 | 10±0.8 | 12±0.5 | 12 ±2 | 12±0.5 | R |

*All the values given as mean± S.D, IMP= Imipenem, CIP= Ciprofloxacin

Table 2: Effect of nanoparticles on HepG2 Cancer cell line

| Cell Viability of HepG2 Cells | | | | | |
|-------------------------------|---------|------------------------------------|----------|-----------|-----------|
| Control | Extract | TiO ₂ NPs Concentration | | | |
| | | 10 µg/mL | 50 µg/mL | 100 µg/mL | 200 µg/mL |
| 98 | 76 | 92 | 84 | 71 | 49 |

**Figure 7.** Cytotoxicity determination by MTT assay against HepG2 cell lines**Table 3.** Coefficients of liver and kidneys after oral exposure to TiO₂ NPs

| Group | Body weight (g) | | | Kidney (mg/g) | Liver (mg/g) |
|------------------------------|-----------------|---------------|---------------|---------------|--------------|
| | Before | After 14 days | After 21 days | | |
| Control | 25 | 30 | 33 | 0.33 ± 2.3 | 1.97 ± 1.3 |
| TiO ₂ (100 mg/kg) | 28 | 31 | 34 | 0.33 ± 4.3 | 2.91 ± 2.3 |
| TiO ₂ (200 mg/kg) | 30 | 35 | 36 | 0.48 ± 1.3 | 2.97 ± 2.3 |

| | | | | | |
|------------------------------|----|----|----|------------|------------|
| TiO ₂ (300 mg/kg) | 24 | 30 | 35 | 0.45 ± 2.3 | 3.47 ± 2.3 |
|------------------------------|----|----|----|------------|------------|

Table 4. Biochemical parameter of mice serum

| | TiO ₂ NPs Concentrations (mg/ml) | Hepatic functions | | | | Renal functions | | |
|---------------|---|-------------------|-----------|-----------|--------------|-----------------|------------|--------------|
| | | ALT (U/L) | AST (U/L) | ALP (U/L) | TBIL (mg/dL) | UA (mg/dL) | CR (mg/dL) | Urea (mg/dL) |
| After 7 days | Control | 30 | 24 | 120 | 0.10 | 3 | 0.53 | 15 |
| | 100 | 33 | 24 | 134 | 0.12 | 6 | 2.3 | 27 |
| | 200 | 36 | 36 | 146 | 0.11 | 5 | 3.3 | 25 |
| | 300 | 40 | 47 | 167 | 0.09 | 4 | 3.7 | 24 |
| After 14 days | Control | 32 | 25 | 123 | 0.12 | 3.5 | 0.6 | 17 |
| | 100 | 35 | 37 | 146 | 0.13 | 7 | 1.1 | 37 |
| | 200 | 38 | 45 | 175 | 0.09 | 5 | 2.2 | 22 |
| | 300 | 43 | 60 | 189 | 0.08 | 4 | 1.8 | 17 |
| After 21 days | Control | 31 | 24 | 115 | 0.11 | 5 | 0.74 | 18 |
| | 100 | 41 | 48 | 190 | 0.15 | 9 | 5.4 | 49 |
| | 200 | 49 | 60 | 206 | 0.13 | 7 | 1.4 | 44 |
| | 300 | 59 | 72 | 234 | 0.10 | 6 | 2.7 | 37 |

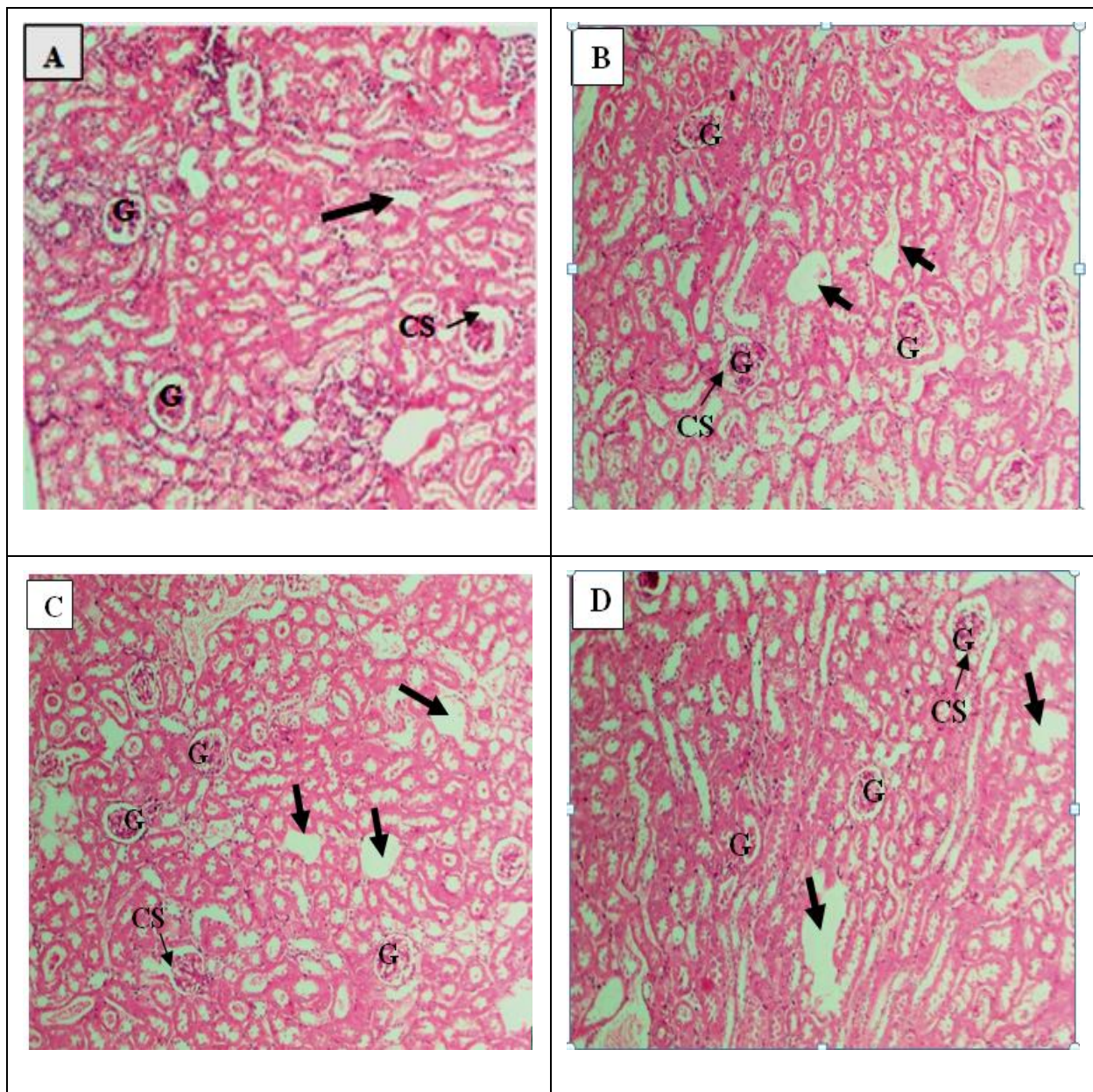


Figure 8. (A-D): Histology of mice kidney after 21 days taken under (10X) treated with TiO₂ NPs

A= Section of the kidney from the control group showing normal glomeruli structure (G), renal capsular space (CS) and normal cellular space (thick arrow) B= Section of the kidney treated with 100mg/kg (low dose) concentration of TiO₂ NPs for 21 continuous days, showing distortion or shrinkage of glomeruli (G) structure, increase in capsular space (CS) and also increase in cellular space (thick arrow). C= Section and D= Section of the kidney treated with 200mg/kg (medium dose) and 300mg/kg (High Dose) concentration of TiO₂ NPs for 21 continuous days, showing distortion and swelling of glomeruli (G) structure, increase in capsular space (CS) and also increase in cellular space (thick arrow), edema formation (cells wash out).

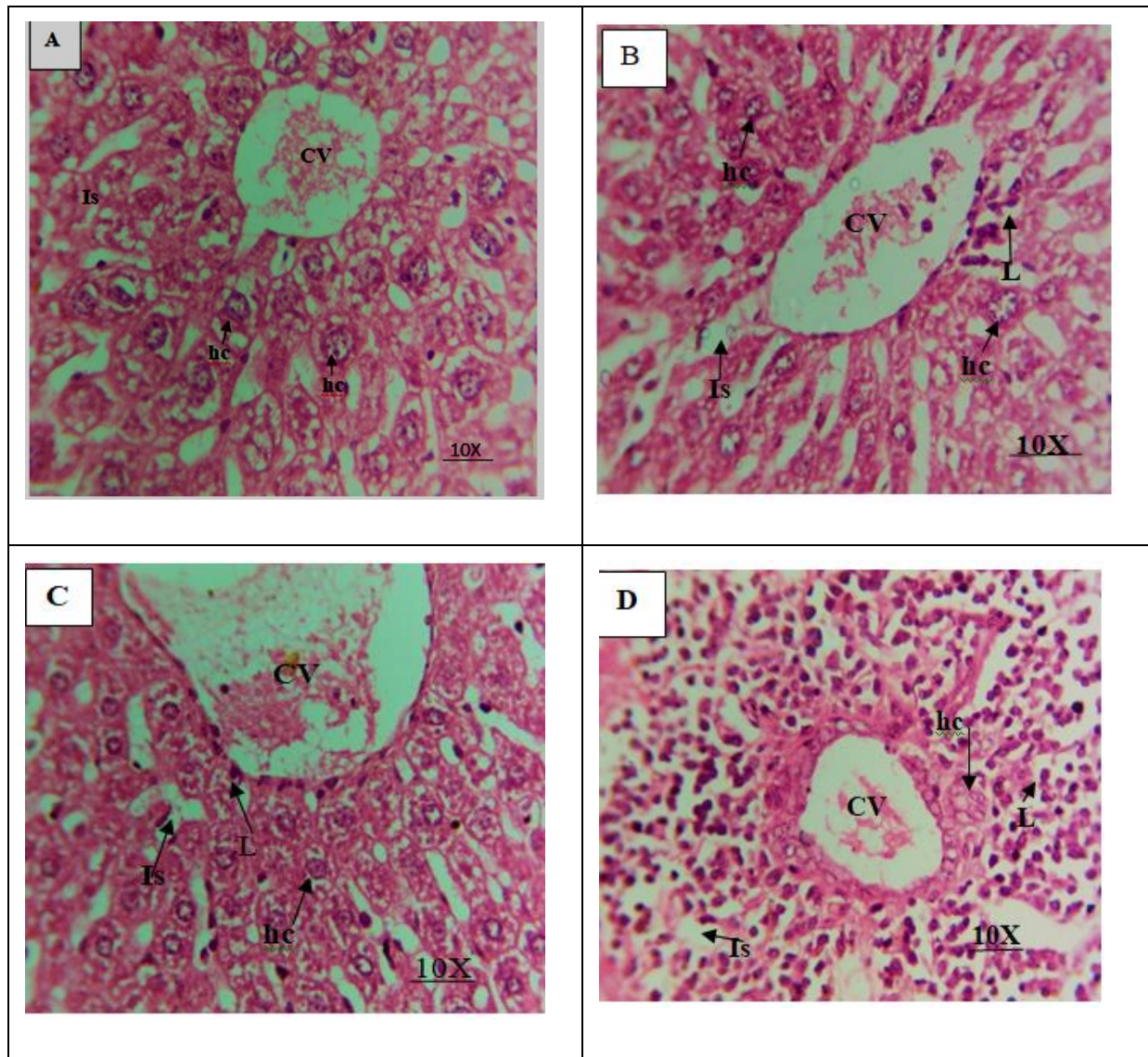


Figure 9. (A-D): Histological analysis of liver following administration of saline solution and TiO₂ NPs for 21days

(A) displaying the normal liver histology of hepatocyte (hc) with binucleated arrangement, prominent central vein (cv) and has eosinophilic cytoplasm (cyt) intervening liver sinusoid (Is) are also shown (B) No significant degeneration of eosinophilic cytoplasm and hepatocyte, except mild infiltration of central vein, liver sinusoid and Leukocyte infiltration (L) examined in mice was exposed to low dose of TiO₂ NPs (C) and (D) Degeneration of eosinophilic cytoplasm, central vein having swelling and infiltration of liver sinusoid was observed in liver of albino mice treated with high dose of TiO₂ NPs.